Biomedical Optics EXPRESS

Miniature objective lens with variable focus for confocal endomicroscopy

Minkyu Kim,[1,2] DongKyun Kang,[1] Tao Wu,[1] Nima Tabatabaei,[1] Robert W. Carruth,[1] Ramses V. Martinez,[3,5] George M. Whitesides,[3,4] Yoshikazu Nakajima,[2] and Guillermo J. Tearney[1,6,7,*]

[1]*Harvard Medical School and Wellman Center for Photomedicine, Massachusetts General Hospital, 55 Fruit Street, Boston, MA 02114, USA*

[2]*School of Engineering, The University of Tokyo, Yayoi 2-11-16 Bunkyo, Tokyo 113-8656, Japan*

[3]*Department of Chemistry and Chemical Biology, Harvard University, 12 Oxford Street, Cambridge, MA 02138, USA*

[4]*Wyss Institute for Biologically Inspired Engineering, Harvard University, 60 Oxford Street, Cambridge, MA 02138, USA*

[5]*Madrid Institute for Advanced Studies, IMDEA Nanoscience, Calle Faraday 9, Ciudad Universitaria de Cantoblanco, 28049 Madrid, Spain*

[6]*Harvard-MIT Division of Health Sciences and Technology, 77 Massachusetts Avenue, Cambridge, MA 02139, USA*

[7]*Department of Pathology, Harvard Medical School and Massachusetts General Hospital, 55 Fruit Street, Boston, MA 02114, USA*

[*]*gtearney@partners.org*

Abstract: Spectrally encoded confocal microscopy (SECM) is a reflectance confocal microscopy technology that can rapidly image large areas of luminal organs at microscopic resolution. One of the main challenges for large-area SECM imaging *in vivo* is maintaining the same imaging depth within the tissue when patient motion and tissue surface irregularity are present. In this paper, we report the development of a miniature vari-focal objective lens that can be used in an SECM endoscopic probe to conduct adaptive focusing and to maintain the same imaging depth during *in vivo* imaging. The vari-focal objective lens is composed of an aspheric singlet with an NA of 0.5, a miniature water chamber, and a thin elastic membrane. The water volume within the chamber was changed to control curvature of the elastic membrane, which subsequently altered the position of the SECM focus. The vari-focal objective lens has a diameter of 5 mm and thickness of 4 mm. A vari-focal range of 240 μm was achieved while maintaining lateral resolution better than 2.6 μm and axial resolution better than 26 μm. Volumetric SECM images of swine esophageal tissues were obtained over the vari-focal range of 260 μm. SECM images clearly visualized cellular features of the swine esophagus at all focal depths, including basal cell nuclei, papillae, and lamina propria.

OCIS codes: (220.3620) Lens system design; (170.1790) Confocal microscopy; (170.2150) Endoscopic imaging; (170.3890) Medical optics instrumentation; (170.2680) Gastrointestinal; (170.4730) Optical pathology.

References and links

1. G. J. Tearney, R. H. Webb, and B. E. Bouma, "Spectrally encoded confocal microscopy," Opt. Lett. **23**(15), 1152–1154 (1998).
2. A. L. Polglase, W. J. McLaren, S. A. Skinner, R. Kiesslich, M. F. Neurath, and P. M. Delaney, "A fluorescence confocal endomicroscope for in vivo microscopy of the upper- and the lower-GI tract," Gastrointest. Endosc. **62**(5), 686–695 (2005).
3. L. Thiberville, M. Salaün, S. Lachkar, S. Dominique, S. Moreno-Swirc, C. Vever-Bizet, and G. Bourg-Heckly, "Human in vivo fluorescence microimaging of the alveolar ducts and sacs during bronchoscopy," Eur. Respir. J. **33**(5), 974–985 (2009).

#224032 - $15.00 USD Received 30 Sep 2014; revised 19 Nov 2014; accepted 19 Nov 2014; published 24 Nov 2014

4. D. Kang, H. Yoo, P. Jillella, B. E. Bouma, and G. J. Tearney, "Comprehensive volumetric confocal microscopy with adaptive focusing," Biomed. Opt. Express **2**(6), 1412–1422 (2011).
5. D. Kang, R. W. Carruth, M. Kim, S. C. Schlachter, M. Shishkov, K. Woods, N. Tabatabaei, T. Wu, and G. J. Tearney, "Endoscopic probe optics for spectrally encoded confocal microscopy," Biomed. Opt. Express **4**(10), 1925–1936 (2013).
6. F. S. Tsai, D. Johnson, C. S. Francis, S. H. Cho, W. Qiao, A. Arianpour, Y. Mintz, S. Horgan, M. Talamini, and Y.-H. Lo, "Fluidic lens laparoscopic zoom camera for minimally invasive surgery," J. Biomed. Opt. **15**, 030504 (2010).
7. A. Divetia, T.-H. Hsieh, J. Zhang, Z. Chen, M. Bachman, and G.-P. Li, "Dynamically focused optical coherence tomography for endoscopic applications," Appl. Phys. Lett. **86**(10), 103902 (2005).
8. M. G. Douali and J. D. Silver, "Self-optimised vision correction with adaptive spectacle lenses in developing countries," Ophthalmic Physiol. Opt. **24**(3), 234–241 (2004).
9. D.-Y. Zhang, V. Lien, Y. Berdichevsky, J. Choi, and Y.-H. Lo, "Fluidic adaptive lens with high focal length tunability," Appl. Phys. Lett. **82**(19), 3171–3172 (2003).
10. H. Oku, K. Hashimoto, and M. Ishikawa, "Variable-focus lens with 1-kHz bandwidth," Opt. Express **12**(10), 2138–2149 (2004).
11. F. S. Tsai, S. H. Cho, Y.-H. Lo, B. Vasko, and J. Vasko, "Miniaturized universal imaging device using fluidic lens," Opt. Lett. **33**(3), 291–293 (2008).
12. J. M. Jabbour, B. H. Malik, C. Olsovsky, R. Cuenca, S. Cheng, J. A. Jo, Y.-S. L. Cheng, J. M. Wright, and K. C. Maitland, "Optical axial scanning in confocal microscopy using an electrically tunable lens," Biomed. Opt. Express **5**(2), 645–652 (2014).
13. B. F. Grewe, F. F. Voigt, M. van 't Hoff, and F. Helmchen, "Fast two-layer two-photon imaging of neuronal cell populations using an electrically tunable lens," Biomed. Opt. Express **2**(7), 2035–2046 (2011).
14. H. Yu, G. Zhou, H. M. Leung, and F. S. Chau, "Tunable liquid-filled lens integrated with aspherical surface for spherical aberration compensation," Opt. Express **18**(10), 9945–9954 (2010).
15. C. Boudoux, S. Yun, W. Oh, W. White, N. Iftimia, M. Shishkov, B. Bouma, and G. Tearney, "Rapid wavelength-swept spectrally encoded confocal microscopy," Opt. Express **13**(20), 8214–8221 (2005).
16. D. Kang, S. C. Schlachter, R. W. Carruth, M. Kim, T. Wu, N. Tabatabaei, P. Vacas-Jacques, M. Shishkov, K. Woods, J. S. Sauk, J. Leung, N. S. Nishioka, and G. J. Tearney, "Comprehensive confocal endomicroscopy of the esophagus in vivo," Endoscopy Int. Open **2**(03), E135–E140 (2014).
17. L. Liu, J. A. Gardecki, S. K. Nadkarni, J. D. Toussaint, Y. Yagi, B. E. Bouma, and G. J. Tearney, "Imaging the subcellular structure of human coronary atherosclerosis using micro-optical coherence tomography," Nat. Med. **17**(8), 1010–1014 (2011).
18. M. Shen, C. Yamahata, and M. A. M. Gijs, "A high-performance compact electromagnetic actuator for a PMMA ball-valve micropump," J. Micromech. Microeng. **18**(2), 025031 (2008).
19. Q. Yang, P. Kobrin, C. Seabury, S. Narayanaswamy, and W. Christian, "Mechanical modeling of fluid-driven polymer lenses," Appl. Opt. **47**(20), 3658–3668 (2008).
20. M. J. Gora, J. S. Sauk, R. W. Carruth, K. A. Gallagher, M. J. Suter, N. S. Nishioka, L. E. Kava, M. Rosenberg, B. E. Bouma, and G. J. Tearney, "Tethered capsule endomicroscopy enables less invasive imaging of gastrointestinal tract microstructure," Nat. Med. **19**(2), 238–240 (2013).
21. M. Gu, *Principles of Three Dimensional Imaging in Confocal Microscopes* (World Scientific, Singapore, 1996).
22. D. Yelin, C. Boudoux, B. E. Bouma, and G. J. Tearney, "Large area confocal microscopy," Opt. Lett. **32**(9), 1102–1104 (2007).
23. D. Shaw and C.-W. Lin, "Design and analysis of an asymmetrical liquid-filled lens," Opt. Eng. **46**(12), 123002 (2007).
24. N. Tabatabaei, D. Kang, T. Wu, M. Kim, R. W. Carruth, J. Leung, J. S. Sauk, W. Shreffler, Q. Yuan, A. Katz, N. S. Nishioka, and G. J. Tearney, "Tethered confocal endomicroscopy capsule for diagnosis and monitoring of eosinophilic esophagitis," Biomed. Opt. Express **5**(1), 197–207 (2014).
25. S. T. Choi, B. S. Son, G. W. Seo, S.-Y. Park, and K.-S. Lee, "Opto-mechanical analysis of nonlinear elastomer membrane deformation under hydraulic pressure for variable-focus liquid-filled microlenses," Opt. Express **22**(5), 6133–6146 (2014).

1. Introduction

Spectrally encoded confocal microscopy (SECM) is a high-speed confocal endomicroscopy technology [1] that can achieve significantly faster imaging speeds than those of other confocal endomicroscopy devices [2, 3]. This high imaging speed of SECM can be utilized to image large areas of tissue by scanning the SECM optics so that the spectrally-encoded line focus traverses the tissue. Previously, large-area confocal microscopy of luminal tissue has been demonstrated with an SECM bench top probe [4]. In this bench top probe, a miniature piezoelectric transducer (PZT) actuator was used to axially translate the objective lens and adaptively change the focus [4]. The adaptive focusing mechanism made it possible to maintain the same imaging depth when the tissue surface was irregular [4]. While the SECM

#224032 - $15.00 USD Received 30 Sep 2014; revised 19 Nov 2014; accepted 19 Nov 2014; published 24 Nov 2014

bench top probe was shown to be capable of successfully conducting adaptive focusing when imaging large areas of the tissue with an irregular surface, the SECM images did not clearly visualize cellular features of the tissue due to the use of a dry-immersion aspheric singlet as the objective lens. Furthermore, the PZT used to control the focus of the bench top probe contains electrical wires, which may be undesirable for certain medical applications.

Recently, we have developed SECM endoscopic probe optics that use a water-immersion aspheric singlet as the objective lens [5]. For these optics, the probe was made watertight, and water was placed between the objective and tissue as an immersion medium. Changing the immersion medium from air to water enabled the visualization of cellular features in tissue [5]. This SECM endoscopic probe, however, was not equipped with an adaptive focusing mechanism, and therefore, some portions of the tissue were not clearly imaged when the tissue was irregular [5]. Incorporating an adaptive focusing mechanism that axially translates the objective lens was not possible with this design, since the objective lens needed to be permanently fixed with the probe housing to achieve water tightness.

One possible solution for adaptive focusing is to use a vari-focal liquid lens inside the watertight SECM probe optics. In this approach, the focus can be changed by hydraulically altering the liquid pressure without moving the objective lens relative to the probe housing. Vari-focal liquid lenses have been successfully used for various imaging applications, including laparoscopic imaging [6], endoscopic optical coherence tomography (OCT) [7] and self-adjustable glasses [8]. However, most vari-focal liquid lenses have relatively low numerical apertures (NA), 0.01 to 0.24 [9–11], which are not suitable for confocal microscopic imaging. High-NA vari-focal lenses have been developed by combining multi-element objective lenses with commercial vari-focal liquid lenses [12, 13]. These high-NA vari-focal lenses have been shown to be capable of conducting microscopic imaging over focal ranges of 225 [12] to 700 μm [13]. The multi-element objective lenses and the commercial vari-focal lenses, however, were relatively large, resulting in a size of 18 × 19.3 × 8.7 mm^3 as the full high-NA lens' dimension [12] and a total diameter of 30 mm [13]. In order for the high-NA vari-focal lens to be utilized in an endoscopic probe, its size must be reduced significantly. Another combinational approach that uses an aspheric singlet in conjunction with a liquid lens has been developed [14], which was shown to reduce spherical aberrations compared to a liquid lens alone. While promising for microscopic imaging, this approach still needs to be evaluated for high-NA microscopic imaging of tissue; its size (about 70 × 25 × 20 mm^3), also needs to be substantially decreased before this approach can be used in endomicroscopic imaging applications.

Here we describe the development and testing of a miniature (5-mm OD) vari-focal objective lens that can be used to conduct adaptive focusing in an SECM endoscopic probe. The miniature vari-focal objective lens was optimally designed to achieve a vari-focal range suitable for adaptive focusing during *in vivo* SECM endoscopic imaging.

2. Methods

2.1 SECM probe optics with a vari-focal objective lens

A schematic of the SECM probe optics with the miniature vari-focal objective lens is shown in Fig. 1A. The SECM probe optics are similar to miniature probe optics that we previously described for an SECM endoscopic probe [5]. Briefly, light from a wavelength-swept source (central wavelength = 1320 nm; bandwidth = 70 nm; repetition rate = 5 kHz) [15] was coupled to a circulator and was delivered to the probe optics through an optical fiber (core diameter = 7.18 μm; core NA = 0.123). In the probe optics, light was collimated by a rod collimation lens (diameter = 2 mm; length = 16 mm; radius of curvature = 5.44 mm) into a 1.9-mm-diameter beam and diffracted by a transmission grating (groove density = 1144 lines/mm). The diffracted light was focused on the tissue by the vari-focal objective lens. Light reflected from the tissue was collected by the same optical fiber and delivered to an

#224032 - $15.00 USD Received 30 Sep 2014; revised 19 Nov 2014; accepted 19 Nov 2014; published 24 Nov 2014

InGaAs photo detector through a circulator. The tissue was mounted on and scanned by a two-axis motorized translation stage to generate two-dimensional SECM images. In future, the probe optics with the vari-focal objective lens will be helically scanned as demonstrated in our previous SECM endoscopic probe [16].

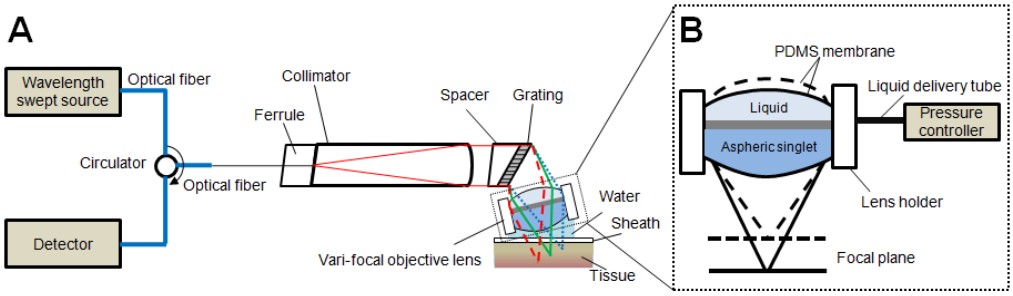

Fig. 1. A – Schematic of SECM probe optics with the miniature vari-focal objective lens. B – Schematic of the vari-focal objective lens.

2.2 Miniature vari-focal objective lens design

Figure 1(B) shows a schematic of the miniature vari-focal objective lens. The vari-focal objective lens was composed of an aspheric singlet and a liquid lens. The liquid was contained in a chamber formed by the top surface of the aspheric singlet, a lens holder, and a thin Polydimethylsiloxane (PDMS) (Dow Corning Sylgard 184) membrane. The liquid volume of the chamber was changed by a syringe mounted on a translation stage from the proximal end, which changed the radius of curvature of the PDMS membrane and subsequently changed the focus.

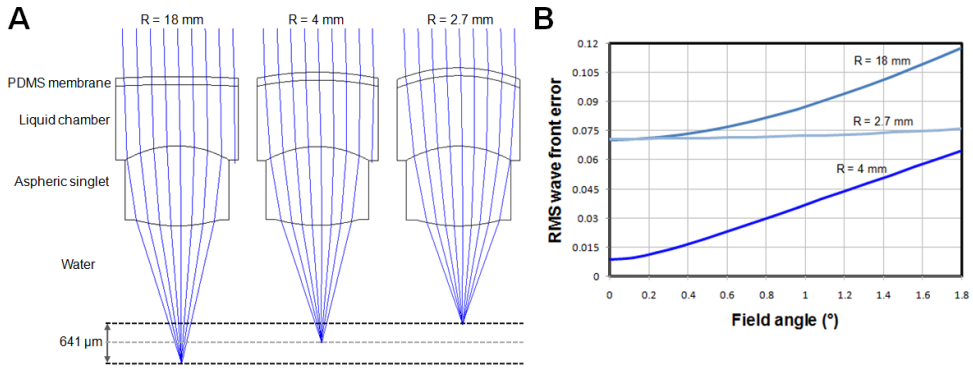

Fig. 2. A – 2D ray tracing layout of the vari-focal objective lens using ZEMAX at three different radii of curvature of PDMS membrane. The focal shift was 641 µm while maintaining diffraction-limited performance. B – RMS wavefront error dependence on the field angle for different radius of curvature of the PDMS membrane.

Key parameters of the vari-focal objective lens were determined through an iterative optimization process using optical simulation software, ZEMAX 13 (Radiant Zemax, WA). Figure 2(A) shows ZEMAX layouts of the vari-focal objective lens at three different PDMS membrane radii of curvature. A custom aspheric singlet (NA = 0.5; water-immersion; focal length = 2.13 mm) that we previously developed for SECM probe optics [5] was used in this vari-focal objective lens. We used ZEMAX simulations to optimized the thickness of the PDMS membrane, refractive index of liquid, and thickness of liquid chamber. For each candidate lens design, the focal shift and RMS wavefront error were simulated at the wavelength of 1320 nm for different values of the radius of curvature of the PDMS membrane. The vari-focal range for each candidate lens was determined as the range of focal

#224032 - $15.00 USD Received 30 Sep 2014; revised 19 Nov 2014; accepted 19 Nov 2014; published 24 Nov 2014

shifts that maintained a diffraction-limited performance (RMS wavefront error less than 0.07) at the center of the field. Figure 2(B) shows RMS wavefront errors as a function of the field angle for the three different radii of curvature. The half field angle of 1.8° corresponded to a full field of view ranging from 100 to 140 μm for the radius of curvature of 2.7 to 18 mm. We calculated the vari-focal range while changing the three design parameters and determined of the optimal values that produced the largest vari-focal range. As the result of this optimization process, the PDMS membrane thickness was set as 250 μm; the liquid refractive index 1.33 (water); and the thickness of the liquid chamber 1 mm. The ZEMAX simulation showed that the resulting vari-focal objective lens has the potential to provide a vari-focal range of 641 μm while maintaining NA of 0.39 to 0.43, when the radius of curvature of the PDMS membrane changes from 2.7 to 18 mm.

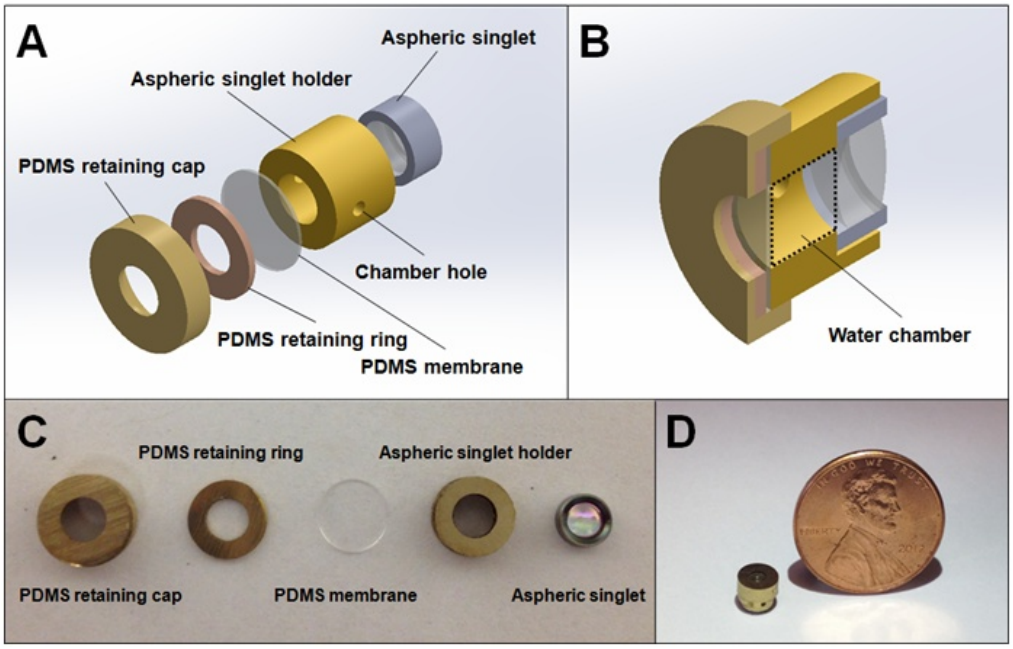

Fig. 3. Mechanical structure and fabrication of vari-focal objective lens. A – exploded view of components of vari-focal objective lens; B – cross sectional view of assembled vari-focal objective lens; C – a photo of components; and D – a photo of the fully-assembled vari-focal objective lens adjacent to a penny for scale.

2.3 Miniature vari-focal objective lens fabrication

We fabricated the vari-focal objective lens using custom-made mechanical parts. Figure 3(A) shows an extruded view of the vari-focal objective lens assembly. A metallic holder (aspheric singlet holder in Fig. 3(A); OD = 4 mm; length = 2.4 mm) was used to hold the aspheric singlet. The proximal surface of the metallic holder was fine polished, as any roughness of this surface could distort the surface profile of the PDMS membrane. The PDMS membrane was fabricated by spin-coating uncured PDMS on a silanized silicon wafer and cured for 20 minutes at 90°C. The cured PDMS was peeled off of the silicon wafer, cut into a 4 mm-diameter disk, and placed on the aspheric singlet holder. A thin metallic ring (PDMS retaining ring; thickness = 0.8 mm) was placed on the PDMS membrane. The bottom surface of the PDMS retaining ring was fine polished to provide uniform contact with the PDMS membrane. Another metallic holder (PDMS retaining cap; OD = 5 mm; length = 2.1 mm) was placed on the PDMS retaining ring. We applied room temperature curing epoxy (7670A22, McMaster-CARR) on the interface between the PDMS retaining cap and aspheric singlet holder and placed the whole assembly under compression while the epoxy was cured. This

#224032 - $15.00 USD Received 30 Sep 2014; revised 19 Nov 2014; accepted 19 Nov 2014; published 24 Nov 2014

method ensured that the PDMS membrane was in stable contact with the surrounding structures.

Figure 3(B) shows a cross-sectional view of the lens assembly. A water chamber was formed between the aspheric singlet and the PDMS membrane. Two small holes (ID = 0.56 mm) were made on the sidewall of the aspheric singlet holder. One of the holes was used as an inlet to change the water pressure inside the chamber. The other hole was used as an outlet to remove air during the initial water filling process.

2.4 Performance test

Mechanical performance: Upon completion of lens fabrication, the cross-sectional profile of the vari-focal objective lens was measured using a high-resolution optical coherence tomography (OCT) system [17]. Water volume was continuously changed while a movie of cross-sectional OCT images (width = 2 mm; height = 0.4 mm) was obtained. The radius of curvature of the PDMS membrane at each OCT image frame was calculated to determine the range of the curvature change.

Optical performance: We used the vari-focal objective lens in conjunction with the collimation optics with a grating that was previously used in the SECM probe optics [5] for testing the performance of the vari-focal objective lens. The lateral resolution of the vari-focal objective lens was measured by imaging a 1951 US Air Force (USAF) resolution target and calculating the full width at half maximum (FWHM) of the line spread function (LSF). The axial resolution was measured as the FWHM of the axial-response curve, an intensity curve obtained by imaging a mirror while axially translating the SECM optics with a motorized stage (VP-25XA, Newport). The peak position of the axial-response curve was used to determine the focal position. Lateral and axial resolutions, field of view, and focal position were measured while varying the water volume. The focal length of the vari-focal objective lens was measured by comparing the field size obtained by the vari-focal objective lens with the field size obtained by the aspheric singlet using a known focal length.

Experimental measurements of lens focusing dynamics: The dynamic performance of the vari-focal objective lens was evaluated by measuring the step response function. The focal plane of the vari-focal objective lens was placed on a mirror, which was tilted at 45° relative to the focal plane. The incidence angle on the vari-focal lens was increased to detect light reflected by the tilted mirror. Due to the 45° tilt angle, a change in focal length was observable as a lateral shift of the maximum-intensity position in the SECM image. The relationship between the focal change and lateral shift was measured by translating the focal plane with a motorized translation stage, and this relationship was later used to convert the lateral shift shown in dynamic SECM images to a focal change. The reflected light from the mirror was laterally shifted when it reached the objective lens. Due to this later shift, the reflected light was not captured by the objective lens at all for a portion of the field of view. This limited the detectable focal change to approximately 120 μm. SECM images were continuously obtained as we applied a step input of volume change that resulted in a steady-state focal shift of 120 μm. For each spectrally-encoded line, the lateral position of the peak was calculated and converted to the focal shift. Since each spectrally-encoded line was sampled at a rate of 5 kHz, due to the repetition rate of the source, we obtained a curve of time versus focal shift sampled at a rate of 5 kHz. We measured the 10% to 90% rise time from this focal shift curve to determine the temporal response of the vari-focal objective lens.

In addition to measuring the temporal response of the lens, we also measured the temporal response of the lens attached to a 1.52 m tube with an ID of 0.86 mm. These tube parameters are based on our current probe designs for imaging the upper gastrointestinal tract, and, as a result,this configuration is a good approximation of how the vari-focal lens will be used once the optics are incorporated into an SECM endoscope. Hydraulic pressure was conveyed through this tube to actuate the vari-focal lens.

#224032 - $15.00 USD Received 30 Sep 2014; revised 19 Nov 2014; accepted 19 Nov 2014; published 24 Nov 2014

Model of lens focusing dynamics: We also calculated a theoretical 3-dB frequency of the vari-focal objective lens by using a simple RLC model developed by Shen et. al [18]. In this approach, the vari-focal objective lens was modeled as a serial circuit of a resistor (water viscosity), an inductor (water inertia), and a capacitor (PDMS membrane stiffiness). Numerical values for the equivalent resistance, inductance and capacitance were calculated by using the Eq. (1) shown in Shen et. al [18] and specific dimensions and properties of our vari-focal objective lens. The stiffness of the PDMS membrane was calculated by a mechanical model of a clamped elastic membrane under pressure described in Yang et. al [19]. These simulations were compared to experimental measurements of the dynamic performance of the vari-focal lens described above.

Determination of the expected depth and temporal tissue variation in the esophagus: In order to determine if our vari-focal objective lens has sufficient focal range and bandwidth for esophageal tissue tracking *in vivo*, we used OCT images of the esophagus obtained from patients with an OCT endoscopic capsule [20]. We estimated the amplitude and frequency of device-to-tissue distance variation from the OCT capsule endomicroscopy cross-sectional images. For each A line, the distance between the outer wall of the OCT capsule and tissue surface was calculated. We plot the device-to-tissue distance versus angle after analyzing the rotational OCT image. For each plot, the standard deviation of the device-to-tissue distance was calculated. The Fourier transform of each plot was calculated, and the frequency at which the amplitude dropped by 3 dB compared to the DC amplitude was determined as 3-dB frequency. The 3-dB frequency indicates the minimum bandwidth that an adaptive focusing system is required to have to follow the device-to-tissue distance variation. We measured the standard deviation and 3-dB frequency for two pull-back image sets, one representing a good tissue contact case and the other a poor tissue contact case.

Tissue imaging performance: Tissue imaging performance was evaluated by imaging excised swine esophageal tissues. Freshly swine esophageal tissue was first treated with 6% concentration acetic acid to enhance the nuclear contrast. The swine tissue then was placed around the SECM focal plane. Large-area SECM images were obtained by raster-scanning the swine tissue with a two-axis translation stage. We changed the water volume to achieve the best axial resolution. During this process, axial resolution was continuously measured while the water volume was changed. When the target axial resolution of 15.9 μm was achieved, the water volume was kept constant and used as the reference point during following water volume change experiments. For the first set of data, the water volume was kept constant, and SECM images from multiple imaging depths were acquired by axially translating the SECM optics with the motorized stage. For the second data set, the SECM focal plane was initially located 120 μm below the tissue surface by using the motorized stage, and the water volume was changed in a stepwise manner while a large-area SECM image was acquired for each water volume change. Once all the data were acquired, the effective imaging depth for a given water volume change was estimated; for each image in the vari-focal data set, a cross-correlation with every image in the stage-scanning data set was calculated. The stage-scanning image that had the largest cross-correlation value was determined as the matching image, and the imaging depth of this stage-scanning image was determined as the effective imaging depth for the given water volume change.

3. Results

3.1 Vari-focal objective lens fabrication

Figure 3(C) shows a photo of the fabricated parts of vari-focal objective lens, and Fig. 3(D) a photo of the assembled vari-focal objective lens. The vari-focal objective lens assembly had an OD of 5 mm and length of 4 mm. The OCT measurement of the lens profile showed that the radius of curvature of the PDMS membrane ranged from 1.85 mm to 7.41 mm.

#224032 - $15.00 USD Received 30 Sep 2014; revised 19 Nov 2014; accepted 19 Nov 2014; published 24 Nov 2014

3.2 Optical and mechanical performance test

Figure 4(A) shows the axial-response curve when the axial FWHM was the smallest, 15.9 µm. The focal length of this configuration was 2.83 mm. The relationship between the focal length and the axial resolution is shown in Fig. 4(B). Over the entire focal range of 240 µm, the axial FWHM was smaller than 26 µm. Figure 5 shows an SECM image of the USAF resolution target when the focal length to the vari-focal objective lens was set at 2.83 mm. The smallest bars (Group 7, Element 6; width = 2.2 µm) were clearly resolved, and the FWHM of the LSF was measured to be 1.84 ± 0.19 µm. The field of view was measured to be 250 µm. When the focal length was increased to 2.88 mm (axial resolution = 26 µm) the lateral resolution and FOV increased to 2.54 ± 0.54 µm and 254 µm, respectively.

Figure 6 shows the dynamic response of the vari-focal objective lens. The 10% to 90% response time for the vari-focal objective lens, t_a, was measured to be 11.4 ± 1.3 ms and the corresponding 3-dB bandwidth was 30.7 Hz. When the 1.52 m long 0.86 mm ID pressure transducing tube was attached to the vari-focal lens, the 10% to 90% response time, t_b, was measured to be 18.1 ± 0.8 ms and the corresponding 3-dB bandwidth of 19.3 Hz.

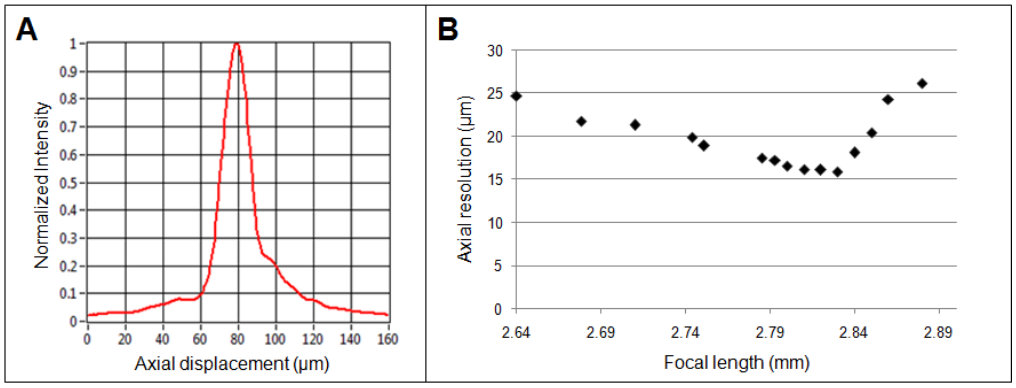

Fig. 4. Axial performance of the vari-focal objective lens. A – an axial response curve at the focal length of 2.83 mm; and B – scatter plot showing the relationship between focal shift and axial resolution.

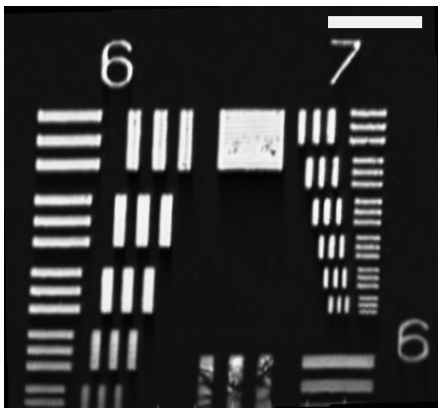

Fig. 5. SECM image of a 1951 USAF resolution target. Scale bar = 50 µm.

From the RLC model calculation, the resistance of the vari-focal lens was estimated as $4.3956\times10^{10}\,Nm^{-5}s$, and the inductance $9.2627\times10^{8}\,kgm^{-4}$. The PDMS membrane had different stiffnesses for different radii of curvature. Thus the capacitance varied from $1.3324\times10^{-14}\,m^{5}N^{-1}$ to $4.9082\times10^{-14}\,m^{5}N^{-1}$ for the varied radius of curvature of 1.85 mm to

#224032 - $15.00 USD Received 30 Sep 2014; revised 19 Nov 2014; accepted 19 Nov 2014; published 24 Nov 2014

7.41 mm. We then simulated the transfer function of the equivalent RLC circuit by using Matlab (Mathworks, MA). From the bode plot of the transfer function, the 3-dB cutoff frequency was found to be 36.6 Hz to 70.3 Hz for the varying PDMS radius of curvature. The measured 3-dB frequency, 30.7 Hz, is similar to these predicted 3-dB frequency values. Similarly, modeling of the lens attached to a 1.52 m long 0.86 mm ID tube provided values that corresponded to our measurements. For this configuration, the modeled 3-dB cutoff frequency was found to range from 20.9 Hz to 41.4 Hz for the varying PDMS radius of curvature, which was consistent with our measure value of 19.3 Hz.

From the analysis of the *in vivo* OCT images of the esophagus, the standard deviation of device-to-tissue distance variation was estimated to be 97 μm, and the 3-dB frequency of device-to-tissue distance variation was 0.55/rotation when the tissue had a good contact with the device. The 3-dB frequency of 0.55/rotation indicates that most of the tissue was located at a constant distance from the device, and small variation of the device-to-tissue distance can be mostly represented by the frequency components between 0 and 0.55/rotation. For the poor tissue contact case, the standard deviation was 520 μm and 3-dB frequency was 1.1/rotation.

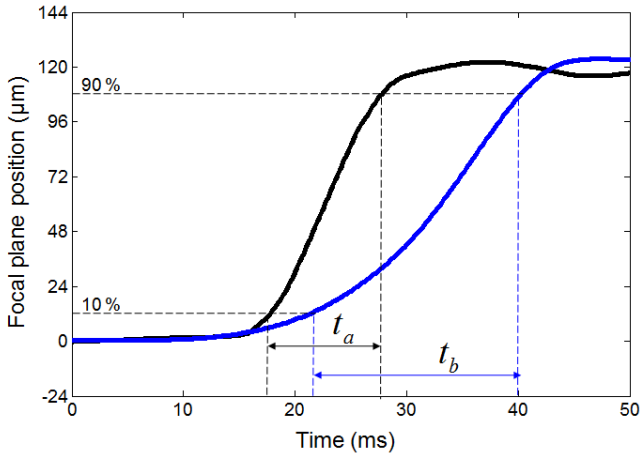

Fig. 6. Step responses of the vari-focal objective lens. black line - vari-focal objective lens; and blue line - vari-focal objective lens with a 1.52 m tube with an ID of 0.86 mm. t_a and t_b show the 10%-90% response times for the vari-focal objective lens w/o and w/ the 1.52 m tube.

3.3 Tissue imaging performance

Figure 7 shows SECM images of the swine esophagus tissue taken from the same transverse location but at different imaging depths. Figure 7(A), 7(C), and 7(E) were obtained by axially translating the vari-focal objective lens, and Figs. 7(B), 7(D), and 7(F) were acquired by changing water volume in the vari-focal objective lens. The image taken at the tissue surface (Fig. 7(A)) appears to exhibit similar morphology, including papillae (arrow), and imaging artifacts (dotted regions) as the image obtained with the water volume change of 0.15 ml (Fig. 7(B)). The image taken at the imaging depth of 120 μm (Fig. 7(C)) appears to reveal similar tissue morphology as the image obtained with the water volume change of 0 ml, Fig. 7(D). Both Figs. 7(C) and 7(D) revealed characteristic cellular features of swine esophagus, enabling the visualization of basal cell nuclei, seen as high-signal dots (circles), and papillae as larger regions with lower signal (arrows). The image taken at the depth of 260 μm (Fig. 7(E)) and the image obtained with the water volume change of −0.18 ml (Fig. 7(F)) also appear to be highly correlated. The cellular features visualized in Fig. 7 were very similar to those shown in SECM images of swine esophagus *ex vivo* and *in vivo* obtained by the SECM endoscopic probe without the vari-focal objective lens [5, 16].

#224032 - $15.00 USD Received 30 Sep 2014; revised 19 Nov 2014; accepted 19 Nov 2014; published 24 Nov 2014

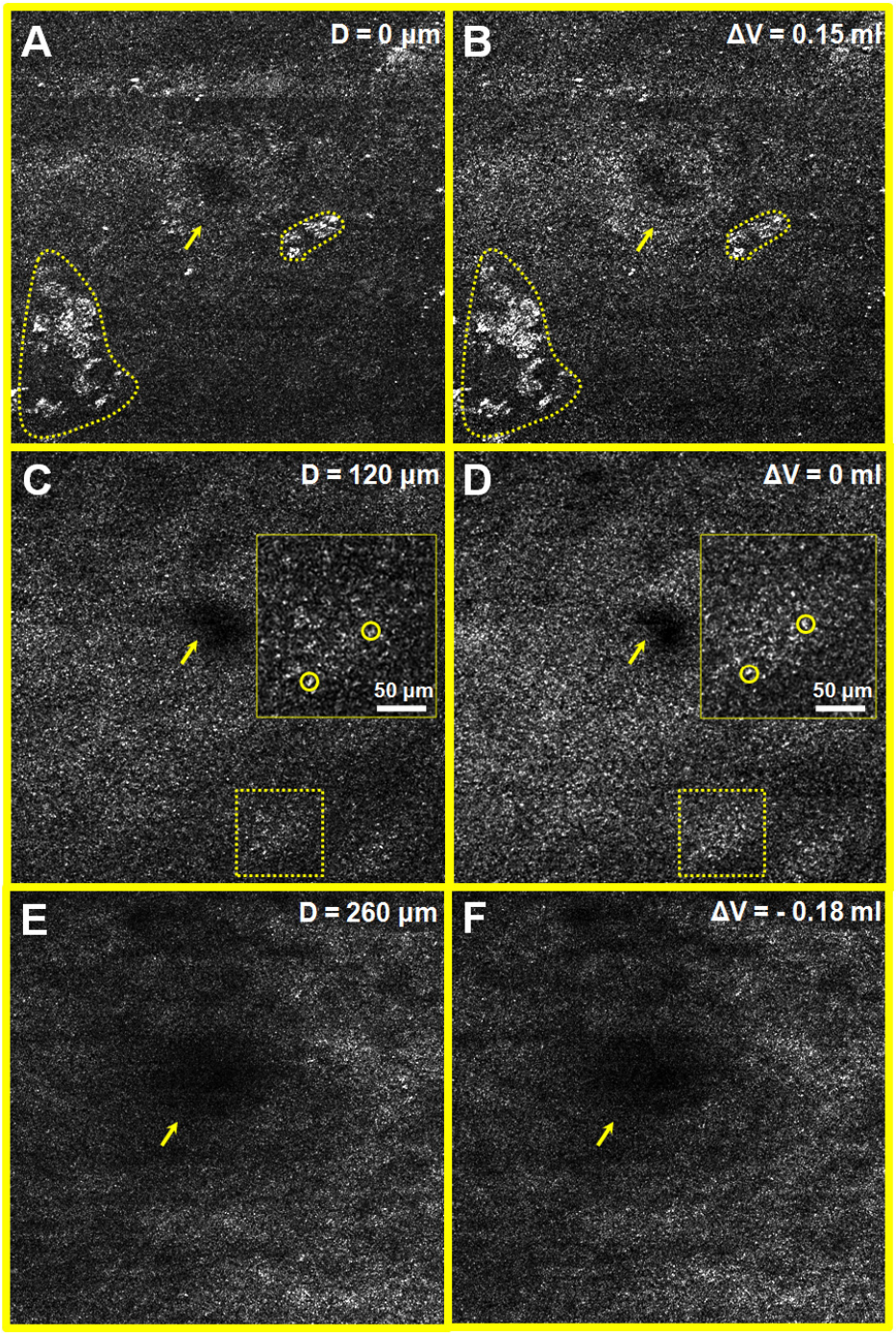

Fig. 7. SECM images of swine esophageal tissue obtained at multiple imaging depths by axially translating the SECM optics (A, C and E) and by changing water volume in the vari-focal objective lens (B, D and F). dotted regions – reflection artifacts originated from scratches on the FEP slip; circles – basal cell nuclei; and arrows – papillae. Size of each image = 1250 µm × 1250 µm.

#224032 - $15.00 USD Received 30 Sep 2014; revised 19 Nov 2014; accepted 19 Nov 2014; published 24 Nov 2014

4. Discussion

In this paper, we have reported the development of a new miniature vari-focal objective lens for confocal endomicroscopy. The lens was designed to change the focus while maintaining a high-NA. The size of the vari-focal objective lens was small, which makes it useful for imaging in small diameter endoscopic probes. The vari-focal objective lens achieved a vari-focal range of 240 μm while maintaining lateral resolution better than 2.6 μm and axial resolution better than 26 μm. SECM images of swine esophagus were obtained over a vari-focal range of 260 μm. All images had sufficient resolution to enable clear visualization of micron-scale features within the tissue.

The measured axial resolution of the vari-focal objective lens, 16 to 26 μm, was poorer than axial resolution of the aspheric singlet alone, 11 μm [5]. The difference in NA, 0.39 – 0.43 for the vari-focal objective lens and 0.5 for the aspheric singlet alone, caused this difference in axial resolution. The measured axial resolution of vari-focal objective lens was also worse than the theoretical axial resolution FWHM of 10.1 to 8.2 μm [21] for the given NA of 0.39 to 0.43. Compared to the theoretical axial response curve, which is square of sinc function [21], the measured axial response curve had relatively slow decrease in intensity. These discrepancies are mainly due to the aberrations generated by deviation of the objective lens shape from the design shape and misalignment between the objective lens and collimator lens. Results from the swine tissue imaging showed that an axial resolution of 16 to 26 μm provides sufficient optical sectioning to visualize cellular features in this tissue type. Since the cells esophageal columnar metaplasia are larger than the 16-26 μm axial resolution, we also expect that the current axial resolution will be sufficient for diagnosing esophageal columnar dysplasia and cancer. Nevertheless, improvements in axial resolution may be required to increase image quality so that a more accurate diagnosis can be made. One simple approach for reducing the optical sectioning thickness is to use shorter wavelengths for SECM imaging [4, 22], which will improve the axial resolution without increasing the effective NA.

The measured vari-focal range, 240 μm, was smaller than the vari-focal range determined from the ZEMAX simulation, 641 μm. There was asymmetric deformation of the PDMS membrane at low water pressure, which was noticeable during OCT measurement of the PDMS membrane profile. The asymmetric PDMS membrane profile can induce additional aberrations and subsequently reduce the useable vari-focal range. The asymmetric PDMS membrane profile was likely caused by uneven compression pressure on the PDMS membrane during the fabrication process, which is consistent with the theoretical and experimental results shown in Shaw et. al [23]. We can ensure that the PDMS membrane has a symmetric profile at low water pressure by monitoring the PDMS membrane profile with OCT while precisely adjusting the compression pressure on the PDMS membrane during the fabrication process.

In our SECM endoscopic probe, the SECM optics is rotated at the rate of 6 revolutions/sec [24]. Therefore, we expect that the SECM optics have the potential to observe a device-to-tissue distance variation with a 3-dB frequency of 3.3 to 6.6 Hz. The measured vari-focal objective lens has a 3-dB cutoff frequency of 30.7 Hz, which is substantially above this range. Even when attached to a 1.52 m long pressure transducing tube, the temporal response was 19.3 Hz. As a result, it is expected that the vari-focal lens will have sufficient bandwidth to follow the tissue surface. The vari-focal range of 240 μm, however, will need to be improved to cover the full range of the device-to-tissue distance variation for poor tissue contact cases. The improvements on the PDMS membrane assembly described before will increase the vari-focal range to the full design value of 641 μm, which will be sufficient for cases in which there is poor tissue contact.

The SECM probe will be rotated during SECM imaging *in vivo* [16], and centrifugal force and gravitational force might affect the optical performance of the objective lens. Choi et. al analyzed effects of gravity on the optical performance of a vari-focal lens that has a similar

#224032 - $15.00 USD Received 30 Sep 2014; revised 19 Nov 2014; accepted 19 Nov 2014; published 24 Nov 2014

aperture diameter to ours, 1.6 mm, and showed that the gravitational effects on optical aberrations become negligible when the PDMS membrane thickness is larger than 90 μm [25]. We therefore expect that the gravitational force will not significantly degrade the optical performance of our vari-focal objective lens that has a PDMS thickness of 250 μm. Centrifugal force applied symmetrically on the PDMS membrane will be symmetric around the optical axis of the vari-focal objective lens since the optical axis is perpendicular to the rotational axis. We therefore expect that any PDMS deformation caused by the centrifugal force can be compensated for by adaptively reducing the water pressure. Pressure and temperature variation on the PDMS membrane can slightly deform the PDMS membrane profile and can subsequently reduce stability of the focal length. In these cases, the PDMS membrane is likely to deform symmetrically, which can be compensated by adaptively changing the water pressure. Dispersion of the PDMS membrane can cause chromatic aberrations. In SECM, different wavelengths are inherently focused onto different locations, and therefore chromatic aberrations should not significantly affect the image quality.

In future research studies with the vari-focal objective lens, we will address the technological issues discussed above to increase the vari-focal range. We will then develop an endoscopic probe that utilizes this vari-focal objective lens for SECM imaging. For this probe, the hydraulic pressure can be controlled by a hydraulic or pneumatic actuator, which can be located at the proximal end of the device.

Acknowledgments

Authors thank Drs. Kengyeh K. Chu, Tim N Ford, Kanwarpal Singh and Manabu Kashiwagi for their assistance in OCT measurement of the lens profile. R. V. M acknowledges funding by the FP7 People program under the project Marie Curie IOF-275148. This research was supported in part through a sponsored research agreement with NinePoint Medical, Cambridge, MA. Dr. Tearney consults for NinePoint Medical. Massachusetts General Hospital has a licensing arrangement with NinePoint Medical. Dr. Tearney has the rights to receive royalty payments as part of this licensing arrangement.